IEEE Access
Multidisciplinary | Rapid Review | Open Access Journal

Received August 7, 2019, accepted August 23, 2019, date of publication August 27, 2019, date of current version September 10, 2019.

Digital Object Identifier 10.1109/ACCESS.2019.2937903

A New Identification Approach of Power System Vulnerable Lines Based on Weighed H-Index

QIAO ZHANG, WENLI FAN, ZIYANG QIU, ZHIGANG LIU, (Senior Member, IEEE), AND JING ZHANG

School of Electrical Engineering, Southwest Jiaotong University, Chengdu 610031, China

Corresponding author: Wenli Fan (fanwenlihp@163.com)

This work was supported in part by the Fundamental Research Funds for the Central Universities under Grant 2682017CX043, and in part by the General Project of Humanities and Social Sciences Research, Ministry of Education, under Grant 18YJCZH028.

ABSTRACT Identification of vulnerable lines in power systems has great meaning to predict cascading failures and prevent the blackouts. A novel approach to identify the vulnerable lines in power systems based on the weighted H-index is proposed. Firstly, to remove the Kirchhoff's law constraint in power system, a second-level correlation network is constructed considering the secondary cascading failure. Then, the relative node strength is defined in the second-level correlation network to improve the identification effectiveness. Secondly, a weighted H-index is proposed, aiming at the disadvantages of the classic H-index only suited for unweighted networks. The improved indicator is applied in the second-level correlation network to identify the vulnerable lines of the power grid. The proposed method is verified in the IEEE-39 bus system and a real-life regional power grid in China. The experimental results show that the proposed method has higher precision compared with other methods. Specifically, the identification accuracy is improved by at least 8.33% than existing methods in the IEEE-39 bus system. In addition, the weighted H-index has higher discrimination and robustness than the classic H-index.

INDEX TERMS Vulnerable lines, weighted H-index, second-level correlation network, power system.

I. INTRODUCTION

In recent years, several blackouts have occurred in the world [1]–[4]. Although these events are not so frequent, every event has a catastrophic impact on the society [5]. The blackouts in Brazil in March 2018 caused about a quarter of consumers to lose power. Due to the overload trip of a bus circuit breaker, the transmitting terminal converter station lose the AC power, and caused bipolar shutdown. In addition, the structure of the Brazilian power grid was unreasonable, which caused the key AC/DC channel from north to south to be affected, which eventually led to the cascading failure. It can be noticed that some critical lines in the system have contributed to the spread of the power outage range. Therefore, searching these vulnerable lines can prevent and block the occurrence of cascading failures effectively.

Great efforts in the identifying or searching vulnerable lines in power systems have been made. The main work can be roughly divided into two categories.

The associate editor coordinating the review of this article and approving it for publication was Md Shihanur Rahman.

The first category is the power system state analysis based on reductionism. It takes the power flow calculation as the core and uses the deterministic or probabilistic method to describe the cascading failure propagation process. Entropy theory, risk assessment theory, and Monte Carlo simulation are introduced to identify the vulnerable lines. In [6], a comprehensive model based on branch power flow transfer entropy and branch flow distribution entropy was established, but it did not consider the influence of branch capacity on the results. Therefore, an incremental power flow entropy model was proposed in [7]. In addition, a line risk index using line overload probability and power flow fluctuations was constructed in [8]. These methods captured the operating state of the system, but they lacked the consideration of the overall system topology. The Monte Carlo simulation method is known for its detailed modeling and accuracy of results. Combinations of components that were likely to cause cascading failures were identified in [9] and [10]. However, due to the dimensionality disaster, the time cost of this method was unacceptable.

The second category method is based on complex network theory. Many network properties (such as small world [11], [12] and scale-free characteristics [13], [14]) and component statistical properties were proposed to analyze the dynamic behavior of the networks. However, the power flow distribution in the power network line is closely related to the line impedance, and does not flow along the shortest path. In addition, the line current connected to the same node is constrained by Kirchhoff's law and has directionality. So, classical complex network theory indicators (such as degree, clustering coefficient and betweenness) do not evaluate the importance of nodes or branches properly. Therefore, electrical indicators were integrated into structural indicators to improve identification accuracy. In [15]–[17] the power transmission distribution factor were used to determine the maximum transmission capacity of the line, thereby reconsidering the line betweenness. And electrical distance were presented in [18]. Subsequently, the electrical betweenness [19], [20], and the flow betweenness [21] were proposed, which considered the utilization on the line between the generator-load pairs. In addition, the maximum flow theory had also been introduced. In [22], the ratio of the flow of the target line to the maximum flow was used to discriminate the importance of the line. In [23], the importance of the line was judged by superimposing the maximum flow in the extreme flow interface. But in fact, the maximum flow method only considers the structural vulnerability of the system, and the operating state system is not fully taken into account. In addition, a load-flow simulation approach was proposed to rank components in availability assessment of multi-state systems [24], [25], which is worth learning in the vulnerable assessment.

Recently, the method of constructing dual graphs based on the cascading failure process has attracted great interest from scholars [26]. Power network structure was modeled as weighted or unweighted undirected graphs, and cascading index, pure and extended spectral metrics were used to assess the vulnerable lines [27]. Further, a correlation network based on N-1 contingency was established in [28]. A more detailed dual graph based on N-1-1 was established in [29]. In [30] and [31], a spatio-temporal correlation graph of the original network was established. A common feature of these graphs is that they are capable of capturing the topological and physical state characteristics simultaneously. In addition, the Kirchhoff's law coupling between the branch states is solved. Based on these graphs, various indicators in complex network theory are applied to identify vulnerable nodes (corresponding to vulnerable lines in the original network). In [32], the impactive and susceptible lines were identified based on the idea of load redistribution. Ma *et al.* [33] applied the PageRank algorithm to screen the vulnerable lines. Structural hole [34], K-shell decomposition [35] had also been applied to the identification of vulnerable lines. In addition, a Bayes network was established to predict the cascading failure propagation based on N-1 contingency [36].

However, the blackouts propagate in the form of cascade faults. The correlation network established by the N-1 contingency [28], [33]–[35] only grasped the first stage of the cascading failure process, the depth of the fault chain was insufficiently grasped, and the vulnerability of the line in the latter failure stage cannot be well quantified, which may result in omissions or misidentifications.

Jorge Hirsch proposed the H-index [37] in 2005, which aimed to quantify the research results as independent individuals. And the H-index was considered to be a major improvement on many of the previous measures, and was widely used to assess the number of academic output and academic research of researchers. Recently, the study in [38] has shown that the degree, H-index and k-shell of network nodes are the initial, intermediate and steady state of the dynamic process, and the H-index is a good trade-off. In many cases, the H-index can quantify the influence of nodes better than the degree and k-shell.

Inspired by the research in [38], an approach based on the weighted H-index to identify the vulnerable lines was proposed. Firstly, a second-level correlation network is constructed in order to overcome the disadvantages of the first-level correlation network constructed in [28] and [33]–[35], which only grasped the first stage of the cascading failure process. Then, to improve the identification effectiveness, the relative node strength is defined in the second-level correlation network. Secondly, a weighted H-index is proposed in order to overcome the disadvantages of the classic H-index only for unweighted networks. Then the improved indicator is applied in the second-level correlation network to identify the vulnerable lines of the power grid. Comparative experiments with existing methods have been conducted in the IEEE-39 bus system and a real-life regional power grid in China. The main contributions are as follows.

- The correlation network that only considers the first-level cascading failure is improved, and a second-level correlation network that considers the secondary cascading failure is established, which can further grasp the dynamic link between the grid branches.
- A weighted H-index indicator is proposed in order to overcome the disadvantages of the classic H-index only for unweighted networks. And the weighted H-index extends the calculation range of the H-index from integer range to the real number range. It improves the identified network type of the indicator, including weighted networks and unweighted networks.

The rest of this paper is organized as below. Section II considers the secondary cascading failure process and establishes a second-level correlation network of the power grid. In section III, we propose the weighted H-index indicator, which is suitable for the identification of node influence in the weighted second-level correlation network. The systematical procedure of the vulnerable lines identification is shown in section IV. The proposed method is verified in the simulations of the IEEE-39 bus system and a regional power grid in China in section V. Finally, conclusions are presented in section VI.

II. CONSTRUCTION OF SECOND-LEVEL CORRELATION NETWORK

In the cascading failure of power systems, the most basic damage to the system is the outage of a single line, because the removal of the node is equivalent to stopping all lines connected to it. Therefore, in order to better reflect the coupling relationship between lines in the power network, reference [35] uses the N-1 contingency to reflect the correlation of the transmission branches on the active power transmission, and constructs the correlation network. However, the blackouts propagate in the form of cascade faults. In most cases, there will be multilevel faults. In [35], only the first-level fault is grasped, and the latter-level faults are ignored. In view of this, a second-level correlation network considering secondary faults is proposed, in order to reflect the power transfer situation and coupling relationship between power lines more deeply without greatly increasing the amount of computation.

In order to take the topology characteristics and the state characteristics into account simultaneously, an improved correlation matrix based on the original power system is proposed.

Step1: Calculate system benchmark power flow and record capacity margins for each line.

Step2: Cut each branch in turn and the power flow increment matrix ΔP is obtained by power increase of other branches caused by the initial fault.

Step3: Judge whether or not the branch power exceeds the limit. If not, the process proceeds to step 4. Otherwise, the element value corresponding to the branch in the matrix ΔP is reserved, then the over-limit branch is broken, the system power flow is calculated again, and the power increment matrix ΔP is updated according to the second power flow increment.

Step4: The improved correlation matrix R is obtained by dividing each element in the power increment matrix ΔP by the capacity margin of the corresponding branch.

According to step 2, the power increment matrix ΔP is shown in (1).

$$\Delta P = \begin{bmatrix} 0 & \Delta p_{12} & \Delta p_{13} & \cdots & \Delta p_{1n} \\ \Delta p_{21} & 0 & \Delta p_{23} & \cdots & \Delta p_{2n} \\ \Delta p_{31} & \Delta p_{32} & 0 & \cdots & \Delta p_{3n} \\ \vdots & \vdots & \vdots & \ddots & \vdots \\ \Delta p_{n1} & \Delta p_{n2} & \Delta p_{n3} & \cdots & 0 \end{bmatrix} \tag{1}$$

where Δp_{ij} is the power increase of branch j after branch i is broken, and n represents the total number of branches in the system.

According to the actual operating characteristics of the power system, the specific elements in (1) are defined [33] as follows.

$$\Delta p_{ij} = \begin{cases} 0, & P_j^i P_j > 0 \,\&\, \left|P_j^i\right| < \left|P_j\right| \\ \left|P_j^i - P_j\right|, & other \end{cases} \tag{2}$$

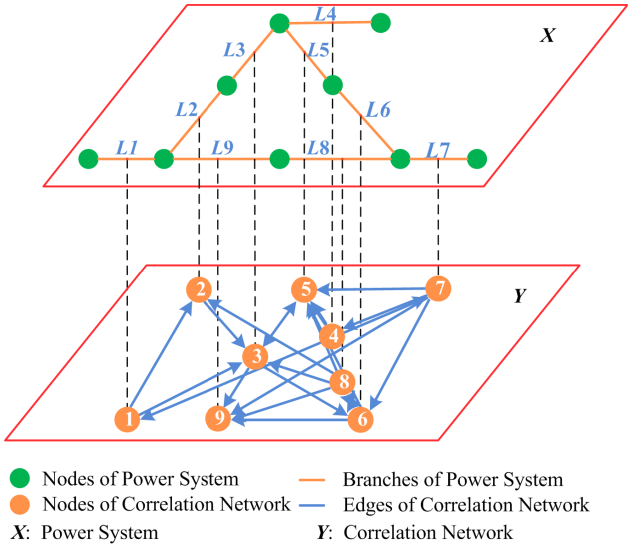

FIGURE 1. A power system and its correlation network.

where P_j^i represents the active power flow of branch j after the breaking of branch i, and P_j represents the initial active power flow of branch j.

The definition of Δp_{ij} in (2) considers the direction of the power flow. 1) When the direction of the power flow is constant, if the branch power flow decreases after the initial fault, the initial fault is considered to have no effect on the line, so Δp_{ij} equals to 0. 2) When the direction is unchanged, if the line power flow increases after the initial fault, or the direction of the power flow changes, Δp_{ij} is considered to be the absolute value of the power flow variation.

Since Δp_{ij} only reflects the absolute influence of the breaking of line i on line j, the capacity margin of line j is not considered, so the degree of interference experienced by line j due to the breaking of line i cannot be fully reflected. In addition, it has no practical significance considering the impact of line breaking on itself. Thus we define the correlation matrix R of the original network in (3).

$$\Delta r_{ij} = \begin{cases} \Delta p_{ij}/M_j, & i \neq j \\ 0, & i = j \end{cases} \tag{3}$$

In (3), Δr_{ij} is the element of matrix R, and it represents the influence of the breaking of line i on line j, M_j represents the capacity margin of line j.

The second-level correlation network corresponding to the original power network can be established based on R. Fig. 1 is a power system and its correlation network. It can be noticed that the branches in the original power network are mapped into nodes in the correlation network, and the edge in the correlation network reflects the coupling relationship between the branches in the original power network vividly. The improved second-level correlation network has better coupling degree than the first-level correlation network established in [35]. And the connection between branches is tighter, which can better reflect the system power transfer in

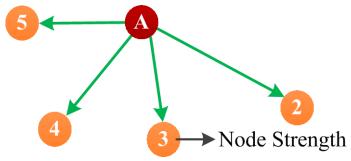

FIGURE 2. Node A and its adjacent nodes.

the process of cascading failures. To sum up, some advantages of the correlation network are highlighted as follow.

1) It reflects the coupling relationship between the branches in the original power network specifically, including the structural and state characteristics.
2) The Kirchhoff's law coupling between the original grid branches is mapped into a general relationship coupling, which facilitates the direct use of complex network theory.
3) Transform the problem of branch vulnerability assessment into a node one.

It can be thoughted that the second-level correlation network captures the first two main processes of cascading failure, and it is a bidirectional weighted network which removes the Kirchhoff's law coupling between the branches in the original power grid. The vulnerability assessment of the branch in power grid is transformed into the evaluation of important nodes in the second-level correlation network, which facilitates the direct application of complex network theory indicators (such as degree, betweenness). The existing literature uses the K-shell decomposition method to identify the influence of nodes in the first-level correlation network [35]. Recent study [38] has shown that the degree, H-index and K-shell are the initial, intermediate and steady state of a dynamic process, and the H-index is a good trade-off. In many cases, H-index can quantify the influence of nodes better than degree and K-shell. However, the classical H-index is only suitable for unweighted networks. Considering that the second-level correlation network is a weighted network, we propose the improved weighted H-index to identify the influence of nodes in the second-level correlation network, which represent the vulnerability of the branches.

III. VULNERABLE LINES IDENTIFICATION BASED ON WEIGHTED H-INDEX

A. CLASSIC H-INDEX

The H-index indicator was proposed by Jorge Hirsch in 2005 [37], which is applied to quantify the research results of researchers as independent individuals and has been widely used in academia. A scientist has index h if h of his or her Np papers have at least h citations each and the other $Np–h$ papers have less than h citations each.

From the perspective of complex networks, the H-index can identify node influence in an unweighted network. As shown in Fig. 2, node A has four adjacent nodes with node strengths of 2, 3, 4, and 5, respectively. Node A has 4 adjacent nodes with strength ≥ 2, and 3 adjacent nodes with strength ≥ 3, but no 4 adjacent nodes with strength≥ 4. According to the definition of H-index, $H_A = 3$.

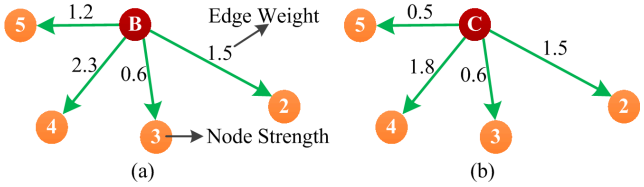

FIGURE 3. Two small weighted networks.

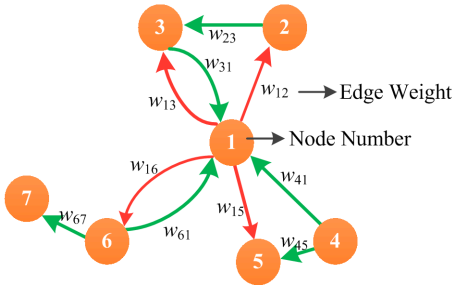

FIGURE 4. Bidirectional weighted network topology.

In fact, most of the networks in real life are weighted networks. Different edge weights have different functions, and the edge weights are not all integers. When the concept of H-index is extended to the correlation network established in this paper, the classical H-index only considers the influence of adjacent nodes, ignoring the importance of edge weights which will reduce the accuracy of vulnerable lines identification. Further more, the calculation result is an integer, which has low discrimination. For example, as shown in Fig. 3, the H-index of nodes B and C are both 3, so the influence of the two nodes cannot be compared. Therefore, this paper proposes a weighted H-index calculation method that considers adjacent nodes and edge weights, which makes it suitable for the identification of node influence in the correlation network. Section *B* shows the specific process.

B. IMPROVED WEIGHTED H-INDEX

It can be noticed from the previous section that the accuracy and recognition of the classic H-index will be reduced when identifying the influence of nodes in weighted networks. However, the second-level correlation network we established is a bidirectional weighted network, so we improve the classic H-index considering the contribution of adjacent node strength and edge weight simultaneously.

First, referring to the definition of node strength in complex networks, only the influence of the target node on its adjacent nodes is considered, and the absolute strength of the node is defined as

$$S_i = \sum_{j \in \Gamma_i} w_{ij} \tag{4}$$

In (4), S_i is the absolute node strength, w_{ij} represents the edge weight pointed by node i to node j, and Γ_i is the set of all adjacent nodes pointed by node i. In the bidirectional weighted network shown in Fig. 4, $\Gamma_1 = \{2, 3, 5, 6\}$.

In the second-level correlation network, the out-degree indicates the influence on its adjacent nodes, and the in-degree indicates the influence of its adjacent nodes on itself. So when defining the absolute strength of a node, we only focus on the impact on other nodes in (4).

In power system, the failure of the target line may cause the power to exceed the limit of other lines. Correspondingly, in the correlation network, the value of w_{ij} will be greater than 1, which increases the risk of cascading failure. Therefore, the *relative node strength* is introduced to define the weighted H-index, as shown in equation (5) and (6).

$$WH_i = \mathcal{WH}\left\{\left(w_{ij}, S_{j|i}\right)_{j\in\Gamma_i}\right\} \tag{5}$$

where

$$S_{j|i} = \left(w_{ij}^{\alpha}\cdot S_j^{\beta}\right)^{\frac{1}{\alpha+\beta}} \tag{6}$$

In (5), WH_i is the weighted H-index of node i. WH is referred to as the calculation operator of weighted H-index. $S_{j|i}$ represents the strength of node j relative to node i. In (6), α and β represent adjustment factors. The node with a larger WH is more vulnerable to its corresponding line.

In the second-level correlation network, the nodes' out-degree indicates the influence on other nodes. The more the number of node's out-degree, the wider the scope of the node's impact. The greater the weight of the node's out-degree, the deeper the influence on its adjacent nodes. Therefore the weighted H-index defined by (5) fully combines the depth and breadth of the node's influence in the system, and has a deeper portrayal of the node's influence. So the weighted H-index reflects the vulnerability of the original network branch in the cascading failure process. Thus, it is reasonable to apply the indicator to identify vulnerable lines of the power grid.

It should be noted that in equation (6), we use geometric mean rather than arithmetic mean to define *relative node strength*. When $w_{ij} > 1$, the multiplicative form can be used to strengthen the strength of the adjacent nodes, and the coupling relationship between the lines can be characterized better. The value of α should not be too small, otherwise the meaning of relative node strength is lost. In addition, when the absolute node strength S_j is close to 0, then the *relative node strength* should also be close to 0. Therefore, in the sense of geometric mean, the appropriate range of values for the parameter α is given as bellow

$$\alpha \in [0.5-\delta, 0.5+\delta] \tag{7}$$

where, δ is a small positive number. We will verify the rationality of the parameter setting range in subsequent simulations.

In Fig. 3, according to equation (5) and (6), the weighted H-index of nodes B and C can be expressed as (here we simply let $\alpha = 0, \beta = 1$).

$$WH_B = \mathcal{WH}\{(1.5, 2), (0.6, 3), (2.3, 4), (1.2, 5)\}$$
$$WH_C = \mathcal{WH}\{(1.5, 2), (0.6, 3), (1.8, 4), (0.5, 5)\}$$

TABLE 1. Weighted H-Index computational process of nodes B and C.

Adjacent nodes order	Node Strength	B			C		
		EW	SEW	WH_{TB}	EW	SEW	WH_{TC}
1	2	1.5	5.6	2	1.5	4.4	2
2	3	0.6	4.1	3	0.6	2.9	2.9
3	4	2.3	3.5	3.5	1.8	2.3	2.3
4	5	1.2	1.2	1.2	0.5	0.5	0.5

Notes: EW is edge weights

Now the problem comes. How to calculate WH_B and WH_C? To solve this problem, we propose an algorithm for computing the weighted H-index of node i as shown in Algorithm1.

The weighted H-index of nodes B and C in Fig. 3 are calculated based on Algorithm 1, and the process is shown in Table 1.

The SEW in Table 1 indicates the sum of the edge weights for all adjacent nodes whose node strength are greater than or equal to the value in the "Node Strength" column. Take node B as an example, it has four adjacent nodes, each of which has a strength of 2, 3, 4, and 5. And the corresponding EW are 1.5, 0.6, 2.3 and 1.2, respectively. For the first adjacent node, the SEW is 1.5+0.6+2.3+1.2=5.6. The temporary weighted H-index of node B (WH_{BT}) equals to $\min\{2, 5.6\} = 2$. After traversing all the adjacent nodes, the final weighted H-index of node B (WH_B) is $\max\{WH_{BTi}\} = 3.5$. Similarly, the final weighted H-index of node A (WH_A) is $\max\{WH_{ATi}\} = 2.9$. It can be seen that the weighted H-index calculation results have a significant difference between node B and node C, rather than the $H_B = H_C = 3$ under the calculation of classic H-index, indicating the effectiveness of the proposed algorithm.

Algorithm 1 Weighted H-Index Calculate

1: Input network parameters
2: **for** $i = 1 : L$(L is the number of nodes)
3: Set WH_i to zero.
4: Calculate the strength of all adjacent nodes of node i
5: Sort all adjacent node strengths of node i in ascending order, get the sequence $S = \{S_{1|i}, S_{2|i}, \cdots, S_{M|i}\}$, M is the length of sequence S.
And the edge weights corresponding to the sequence S is $W = \{w_{i1}, w_{i2}, \cdots, w_{iM}\}$.
6: **for** $k = 1 : M$
7: $SUMW_k = \sum_m w_{in}\ s.t.\ w_{in} >= w_{ik}$.
8: $WH_{Ti} = min\{S_{k|i}, SUMW_k\}$.
9: $WH_i = max\{WH_i, WH_{Ti}\}$.
10: **end for**
11: **end for**

In fact, the classic H-index is a special case of the weighted H-index, that is, all the edge weights in the classic H-index are 1. In Fig. 2, the weighted H-index of node A can be expressed by equation (5) as

$$WH_A = \mathcal{WH}\{(1, 2), (1, 3), (1, 4), (1, 5)\}$$

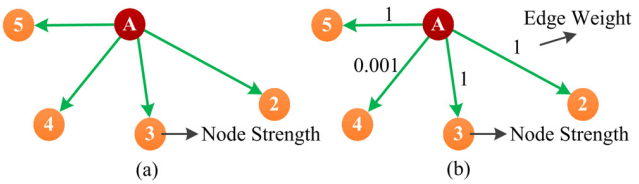

FIGURE 5. Node A and its adjacent nodes with small weight.

According to the proposed algorithm, the calculation result is still $WH_A = 3$.

The weighted H-index also improves the robustness of the classic H-index. Specifically, in Fig. 5(a), node A has four adjacent nodes with node strengths of 2, 3, 4, and 5, respectively. From the perspective of classic H-index, $H_A = \mathcal{H}\{2, 3, 4, 5\} = 3$. The weights of edges are ignored (as shown in Fig.2(b), the weight 0.001 indicates weak link between the two nodes), which will not detect the presence of small-weight, high-strength nodes and lead to a misleading results. Therefore, in order to overcome this defect, we proposed the weighted H-index algorithm in Algorithm 1. In the new algorithm, the weights of every edge will be compared. Small weights can only make a weak contribution to the final weighted H-index. For instance in Fig.5(b), the weight of node 4 (0.001) can be regarded as a disturbance. Under the calculation of classic H-index, the $H_A = 3$. If the weight 0.001 is deleted, $H_A = 2$, which is significantly different from the original. However, in the calculation of the weighted H-index, $WH_A = \mathcal{WH}\{(1, 2), (1, 3), (0.001, 4), (1, 5)\} = 2.001$. Further more, if the weight 0.001 is deleted, $WH_A = \mathcal{WH}\{(1, 2), (1, 3), (1, 5)\} = 2$, which can't be affected by the weak weight (disturbance). Thereby, it can be noticed that the algorithm will automatically filter out low-weight edges (disturbance) but the classic H-index can't. So the weighted H-index will not be affected by small-weight, high-strength nodes like the node 4 in Fig.2(b) which could be regarded as a disturbance. Therefore the system's robustness is improved.

Therefore, by the (5) for the weighted H-index and the proposed weighted H-index algorithm, a weighted H-index calculation method suitable for real-number ranges can be obtained, which can be used for node influence calculation in *second-level correlation network* (even all weighted networks) and has a higher discrimination and robustness than the classic H-index.

IV. VULNERABLE LINES IDENTIFICATION PROCEDURE

According to the previously established second-level correlation network and weighted H-index algorithm, a systematical network vulnerable lines identification procedure is proposed.

Step1: Obtain the basic parameters of the power network and calculate the benchmark power flow.

Step2: Construct an improved correlation matrix R of the original power system according to the correlation matrix establishment method proposed in Section II. The improved *second-level correlation network* is constructed mapping the line in the original power system into a node, and take the elements in the correlation matrix R as edge weights.

Step3: Calculate the weighted H-index for each node according to (5) (6) and the weighted H-index calculation algorithm proposed in section III.

Step4: Sort the node weighted H-index in descending order using the calculation results in step4, and the node number corresponds to the line number in the original power system. The node with a larger weighted H-index means that the corresponding line in the original grid is more vulnerable.

V. CASE STUDY

A. VERIFICATION INDICATOR

Line vulnerability attack research can be applied to identify faults that have a serious impact on the system. The general method is to selectively remove certain lines from the network, and then take the decline of the network performance as a measure of the line vulnerability. The metrics include netability [16], system load loss, and so on. Vulnerability attacks mainly include random line attacks, static deliberate attacks, and dynamic attacks.

In the cascading failure simulation study in [39], based on the DC OPA model, the slow dynamic process is neglected, and the heavy-duty trip and hidden faults are considered, and the physical characteristics of the grid are characterized more deeply and meticulously. On this basis, the AC OPA model is applied to perform static deliberate attacks on the lines in the order of line numbers. The vulnerable lines identified by the weighted H-index algorithm are verified. The number of simulations is set to N times, and the average load loss after each line is attacked is counted, as shown in (8). The larger the value of $P_{loss}(n)$, the more vulnerable the line is. And the order of the vulnerable lines derived from P_{loss} is called *cascading failure simulation*(CFS) ordering [40].

$$P_{loss}(n) = \frac{\sum_{n=1}^{N} p_{loss}(n)}{N} \tag{8}$$

In (9), $P_{loss}(n)$ is referred to as the average load loss of the system after the attack of the line n, $p_{loss}(n)$ represents the system load loss after the line n after each attack, and N is the number of attacks.

B. IEEE-39 BUS SYSTEM

The IEEE-39 bus system is a transmission network in New England, USA, consisting of 39 nodes, 46 branches, and 10 generators, of which generator 31 is a balancing machine.

In CFS, the number of simulations is set to 10000, and the average load loss with each line as the initial fault is obtained. Based on this, the validity of the proposed method is verified.

The first m lines identified by the proposed method are compared with the first m lines in the CFS order. If there are k lines that match the CFS, then we define the identification accuracy as k/m. Table 2 shows the comparison between the identification results of weighted H-index(WH) and the first 12 lines of the CFS ranking results when $\alpha = 0.5$. The second

TABLE 2. Weighted H-Index Identification Results in IEEE-39 bus system.

Rank	CFS	*WH*	VD
1	46	14	3.328
2	38	28	2.673
3	35	38	2.628
4	14	*13	2.628
5	28	20	2.588
6	20	18	2.572
7	37	19	2.571
8	18	*23	2.571
9	39	35	2.548
10	32	37	2.515
11	33	33	2.457
12	19	39	2.302
Accuracy	——	**10/12**	——

Notes: The line with the * is the line with the wrong identification.

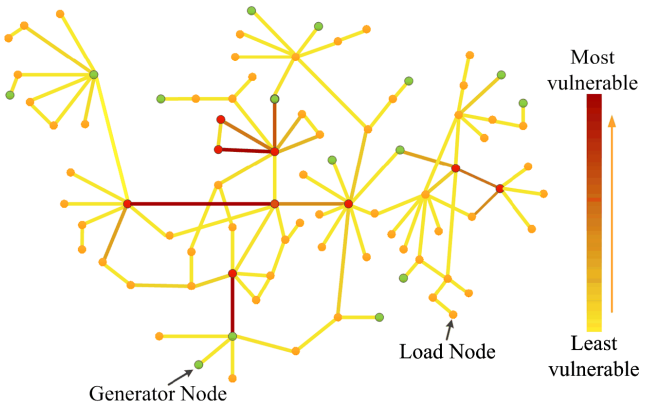

FIGURE 6. Schematic diagram of line vulnerability distribution.

TABLE 3. Comparison of identification accuracy of different methods.

Rank	CFS	*WH*	*WH*_1	*MF*	*IMF*	*PRA*	*CEI*
1	46	14	35	26	10	46	35
2	38	28	14	37	33	37	14
3	35	38	13	30	14	39	23
4	14	13	19	33	20	35	20
5	28	20	23	29	5	33	37
6	20	18	18	38	46	34	33
7	37	19	20	27	41	38	13
8	18	23	38	7	39	41	19
9	39	35	37	36	11	45	38
10	32	37	33	20	34	42	39
11	33	33	42	6	3	44	28
12	19	39	39	39	27	20	34
Accuracy	——	**10/12**	**9/12**	**5/12**	**5/12**	**7/12**	**9/12**

column is the result of CFS sorting, and the third column is the sorting result of *WH*. There are 10 lines that match the two, so the accuracy is 10/12=83.33%. The vulnerable degree (VD) is list in the fourth column. Lines 13, 23 are lines identified incorrectly.

In order to further verify the identification effect of the proposed method, *WH* is compared with the existing methods.

- Apply the weighted H-index to the first-level correlation network (*WH*_1).
- The maximum flow method (*MF*) [22].
- The improved maximum flow method (*IMF*) [23].
- PageRank algorithm (*PRA*) [33]
- Cascading index (*CEI*) [27], [41]

Table 3 shows the comparison of the first 12 lines of the different methods. From the perspective of accuracy, the identification accuracy of *WH* is higher than that of other methods. On the one hand, the accuracy of using the weighted H-index in the second-level correlation network is higher than that in the first-level correlation network, indicating the effectiveness of the improvement to the first-level correlation network. On the other hand, no matter the weighted H-index is used in the second-level correlation network or the first-level correlation network, the identification accuracy is higher than that of *MF*, *IMF* and *PRA*. It is worth noting that *CEI* was originally a vulnerability indicator, and its sorting result is very similar to that of *WH*. Only one of the first 12 lines is different. In the case of system load shedding (CFS) as a verification indicator, *WH* is slightly better than *CEI*. That is to say, the method proposed in this paper can describe the power flow transformation more accurately after the line is attacked. Attacking the lines identified by the method proposed in this paper makes it easier for the system to approach the self-organized critical state.

In addition, we further compared *WH* with pure and extended spectral vulnerable metrics under N-1 contingency proposed in [27]. We choose the two different weights of f_l (power flow in the line) and PR_l (line percentage of rating, different from the PageRank algorithm in [33]) for each line. Under each weight, the four spectral metrics, the natural connectivity (λ), the effective graph resistance (R), the spectral radius (ρ) and the algebraic connectivity (μ_2) are calculated separately, and the identification results are shown in Table 4. Overall, the accuracy of *WH* indicator is higher than that of pure and extended vulnerable metrics. It can be observed that the spectral metrics based on the weight f_l failed to identify the vulnerable lines. This can be explained as the f_l-based indicators ignore the line capacity. The identification results of *WH* and spectral radius indicators are close, but *WH* is slightly better than the spectral radius(ρ) metric.

In summary, in the comparison with other literature methods as mentioned above, the effectiveness of the proposed WH method has been verified, and the identification accuracy is higher than other methods. Specifically, the identification accuracy is improved by at least 10/12-9/12=8.33%.

C. REAL-LIFE REGIONAL POWER GRID OF CHINA

This section analyzes a regional power grid in China as an example. The system has 86 nodes, 100 branches, 15 generators. For convenience, we call the grid the CQ grid here.

Table 4 lists the comparison of the identification results of the proposed method ($\alpha = 0.5$) in the CQ grid with the CFS ordering. In the first 10 lines, the weighted H-index identification results are consistent with the CFS ranking results with an accuracy of 80%. Among them, lines 23 and 89 are identified incorrectly, but their rankings are close to the bottom, 7th and 8th respectively.

TABLE 4. Comparison of WH and spectral metrics under the weight of f_l and PR_l.

Rank	CFS	*WH*	*WH*_1	f_l				PR_l			
				λ	R	ρ	μ_2	λ	R	ρ	μ_2
1	46	14	35	23	29	23	29	35	23	35	23
2	38	28	14	35	36	35	36	14	14	23	9
3	35	38	13	12	23	12	23	46	12	38	4
4	14	13	19	19	24	19	24	23	11	14	14
5	28	20	23	38	20	38	9	38	37	19	37
6	20	18	18	9	17	9	4	19	4	20	11
7	37	19	20	10	1	10	1	13	33	13	19
8	18	23	38	15	16	15	20	42	9	37	6
9	39	35	37	11	14	11	14	33	1	18	33
10	32	37	33	1	4	1	17	37	6	33	25
11	33	33	42	8	37	8	37	10	39	28	12
12	19	39	39	26	12	26	33	20	7	42	39
Accuracy	——	**10/12**	**9/12**	**3/12**	**3/12**	**3/12**	**4/12**	**8/12**	**4/12**	**9/12**	**5/12**

TABLE 5. Weighted H-Index identification results in CQ grid.

Rank	CFS	*WH*	VD
1	16	16	3.80
2	33	33	3.80
3	27	30	3.71
4	30	27	2.50
5	29	90	2.17
6	14	29	2.03
7	25	*23	1.74
8	26	*89	1.72
9	90	14	1.43
10	72	72	1.33
Accuracy	——	**8/10**	——

Fig. 6 is a schematic diagram of the vulnerability distribution of the grid lines with geographic information. The darker the color, the higher the vulnerability of the line. As can be seen, most of the lines have very low vulnerability, but a small number of lines have very high vulnerability. Lines 16 and line 33 have a vulnerability of 3.8, with the highest degree of vulnerability in this area. These two lines are the highest voltage 220kV double-circuit transmission lines in the system, and line 16 is the key connection line connecting the east and west subnets. Line 33 ensures that the power of the connected generator can be normally delivered. If lines 16 and 33 are attacked, a large range of power flow will be caused, and even a cascading failure will occur.

Next we will compare the identification results with other approaches mentioned in section *B*, electrical distance [18] and random results. Top 6 lines are selected from the above method and removed from the system sequentially. The remaining load is calculated shown in Fig. 7. After continuously attacking 6 lines according to the identification result of *WH*, the residual load of the system is less than 60%, which can be considered as a very large power blackout. After continuously attacking 6 lines according to the *IMF* identification result, the system residual load is 70%, and randomly selecting the line to attack the network has almost no impact on the system. The simulation results show that the system is more sensitive to the weaker lines identified in this paper than the other methods, and these lines should be protected in a focused manner.

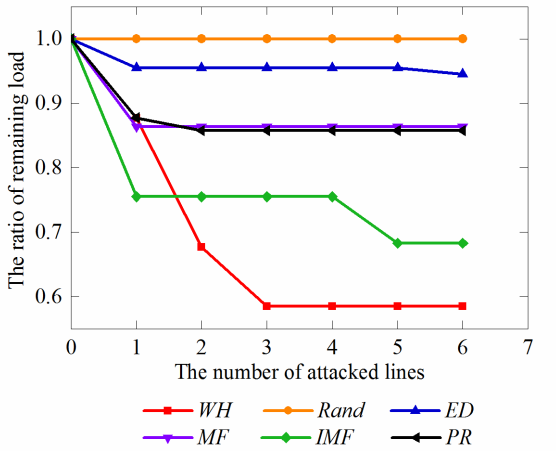

FIGURE 7. System residual load under different removal strategies.

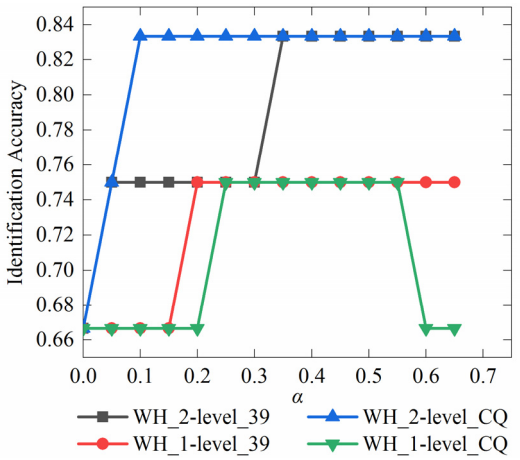

FIGURE 8. Identification accuracy under different α.

D. ANALYSIS OF THE INFLUENCE OF PARAMETER α ON IDENTIFICATION RESUILTS

Fig. 8 shows the variation of the identification accuracy with the parameter α using the proposed method in two cases.

It can be observed from Fig. 8 that the influence of the parameter α on the identification accuracy tends to change stepwise. That is, the accuracy remains constant within a certain range. With α changes, the overall accuracy remains

TABLE 6. Algorithm time consumption in IEEE-39 bus system and CQ grid.

Case	IEEE-39 bus system			CQ grid		
Methods	WH_1-level_39	WH_2-level_39	CFS_39	WH_1-level_CQ	WH_2-level_CQ	CFS_CQ
Time cost	3.554770s	3.966335s	12179.61s	5.676405s	9.349052s	34327.24

Notes: "WH_x-level_39" indicates that the weighted H-index is applied to the x-level correlation network of the IEEE-39 node system, x=1,2. "H_x-level_CQ" indicates that the classic H-index is applied to the x-level correlation network of the CQ grid.

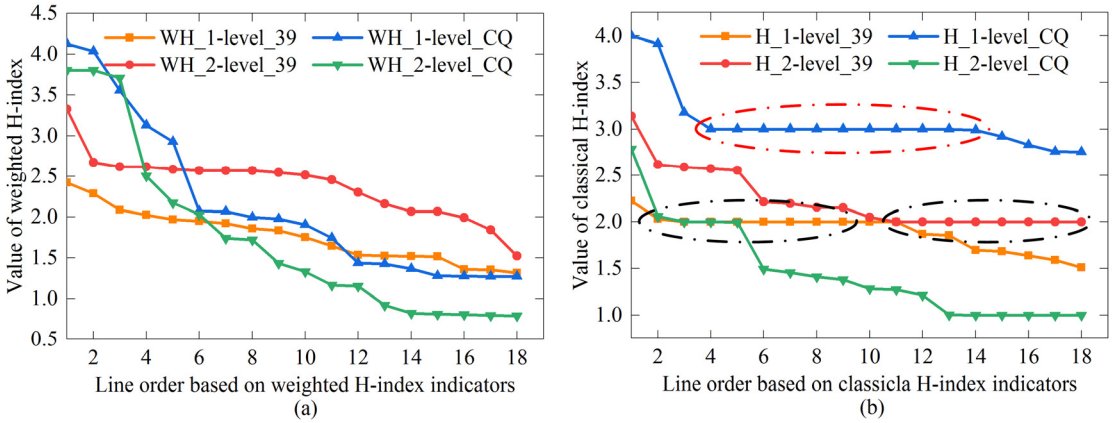

FIGURE 9. Discrimination comparison between the weighted H-index and the classic H-index. (a) Weighted H-index identification results, where "WH_x-level_39" indicates that the weighted H-index is applied to the x-level correlation network of the IEEE-39 node system, x=1,2. (b) Classic H-index identification results, where "H_x-level_CQ" indicates that the classic H-index is applied to the x-level correlation network of the CQ grid.

between 0.67 and 0.83. When α is less than 0.3, the accuracy is relatively low, and without exception, when α is taken as 0, the accuracy is the lowest. At this time, the equation (5) uses the absolute node strength in the correlation network rather than the relative, which illustrates the effectiveness of the *relative node strength* proposed in this paper. When $0.4 < \alpha < 0.55$, the identification accuracy is the highest, indicating that the parameter range given in (7) is reasonable. In addition, regardless of how α changes, the weight H-index is more accurate in the second-level correlation network than in the first-level correlation network. It shows the effectiveness of this paper on the improvement to the first-level correlation network.

E. TIME COMPLEXITY ANALYSIS OF THE ALGORITHM

The computational complexity of the first and second-level correlation networks varies with the network, and the establishment time of the second-level correlation network is greater than that of the first. Specifically, in the two test networks of this paper, the time consumed by the identification algorithm based on the first and second-level correlation networks is shown in Table 6. It can be noticed from the Table 6 that the algorithm consumption time based on the second-level correlation network is greater than that on the first. When the network size is larger, the difference between the two is larger, but both are within an order of magnitude. In addition, the time consumed by the method is much less than the calculation time of the verification indicator CFS. Therefore, the calculation time of the method based on the second-level correlation network is acceptable. When using a server with better performance, the algorithm consumption time will be further shortened, and it is expected to realize online application.

F. COMPARISON OF THE DISCRIMINATION BETWEEN WEIGHTED H-INDEX AND CLASSIC H-INDEX

Aiming at the shortcomings of the classic H-index identification, we use the weights of the edges to improve the solution process of the classic H-index. In order to compare the effects before and after the improvement, the weighted H-index and the classical H-index (*CH*) are applied to identify the vulnerable lines in the IEEE-39 bus system and the CQ grid according to the first-level and second-level correlation network. The results are shown in Fig. 9. In Fig. 9(b), the *CH* values will remain constant within a certain range whatever in which system or correlation network. That is, the vulnerability of these lines is the same. The *CH* does not distinguish these lines' vulnerability. In contrast, in Fig. 9(a), the *WH* values decrease in turn as the order of the lines increases, and have a high discrimination for each line. This shows the effectiveness of this paper on the improvement of the classic H-index.

VI. CONCLUSION

This paper proposes a method based on weighted H-index for vulnerable lines identification. Two major contributions are made to existing methods. Firstly the correlation network that only considers the first-level cascading failure [33]–[35]

is improved, and a second-level correlation network that considers the secondary cascading failure is established, which can further grasp the dynamic link between the grid branches and transforms the branch vulnerability assessment problem into an easy-to-handle node one cleverly. The second-level correlation network can further grasp the topological and electrical characteristics of the power system more fully than the traditional reduction-based analysis method [22], [23]. Secondly a weighted H-index indicator is proposed in order to over-come the disadvantages of the classic H-index only for unweighted networks. In addition, the weighted H-index extends the calculation range of the H-index from integer range to the real number range. It improves the identified network type of the indicator, including weighted networks and unweighted networks.

In fact, the proposed weighted H-index can be used not only for power grid, but also suitable for other weighted networks such as water pipeline networks, energy transport networks, and the like.

Although the correlation network considering the secondary fault has higher identification accuracy than the correlation network only considering the primary fault, there are still two lines of misunderstanding in the first 10 lines, which demonstrates the complexity of the mechanism of cascading failure propagation. Therefore how to further improve the identification accuracy will be the focus of our future work.

REFERENCES

[1] H. Guo, C. Zheng, H. H.-C. Iu, and T. Fernando, "A critical review of cascading failure analysis and modeling of power system," *Renew. Sustain. Energy Rev.*, vol. 80, pp. 9–22, Dec. 2017.

[2] A. Muir and J. Lopatto, "Blackout 2003: Final report on the August 14, 2003 blackout in the United States and Canada: Causes and recommendations," Tech. Rep., 2004.

[3] L. L. Lai, H. T. Zhang, C. S. Lai, F. Y. Xu, and S. Mishra, "Investigation on July 2012 Indian blackout," in *Proc. Int. Conf. Mach. Learn. Cybern.*, Jul. 2013, pp. 92–97.

[4] O. P. Veloza and F. Santamaria, "Analysis of major blackouts from 2003 to 2015: Classification of incidents and review of main causes," *Electr. J.*, vol. 29, no. 7, pp. 42–49, 2016.

[5] B. Appasani and D. K. Mohanta, "A review on synchrophasor communication system: Communication technologies, standards and applications," *Protection Control Mod. Power Syst.*, vol. 3, no. 1, p. 37, Dec. 2018.

[6] Y. Li, J. Liu, X. Liu, L. Jiang, Z. Wei, and W. Xu, "Vulnerability assessment in power grid cascading failures based on entropy of power flow," *Automat. Electr. Power Syst.*, vol. 36, no. 19, pp. 11–16, 2012.

[7] R. Fang, R. Shang, Y. Wang, and X. Guo, "Identification of vulnerable lines in power grids with wind power integration based on a weighted entropy analysis method," *Int. J. Hydrogen Energy*, vol. 42, no. 31, pp. 20269–20276, Aug. 2017.

[8] X. Li, X. Zhang, L. Wu, P. Lu, and S. Zhang, "Transmission line overload risk assessment for power systems with wind and load-power generation correlation," *IEEE Trans. Smart Grid*, vol. 6, no. 3, pp. 1233–1242, May 2015.

[9] M. J. Eppstein and P. D. H. Hines, "A 'random chemistry' algorithm for identifying collections of multiple contingencies that initiate cascading failure," *IEEE Trans. Power Syst.*, vol. 27, no. 3, pp. 1698–1705, Aug. 2012.

[10] P. Rezaei, P. D. H. Hines, and M. Eppstein, "Estimating cascading failure risk: Comparing Monte Carlo sampling and random chemistry," in *Proc. IEEE PES Gen. Meeting Conf. Expo.*, National Harbor, MD, USA, Jul. 2014, pp. 1–5.

[11] D. J. Watts and S. H. Strogatz, "Collective dynamics of 'small-world' networks," *Nature*, vol. 393, no. 6684, pp. 440–442, 1998.

[12] T. Xu, R. Chen, Y. He, and D. R. He, "Complex network properties of Chinese power grid," *Int. J. Mod. Phys. B*, vol. 18, nos. 17–19, pp. 2599–2603, Jul. 2004.

[13] R. Albert, H. Jeong, and A.-L. Barabási, "Error and attack tolerance of complex networks," *Nature*, vol. 406, pp. 378–382, Jul. 2000.

[14] A.-L. Barabási and R. Albert, "Emergence of scaling in random networks," *Science*, vol. 286, no. 5439, pp. 509–512, 1999.

[15] E. Bompard, R. Napoli, and F. Xue, "Analysis of structural vulnerabilities in power transmission grids," *Int. J. Critical Infrastruct. Protection*, vol. 2, nos. 1–2, pp. 5–12, 2009.

[16] E. Bompard, R. Napoli, and F. Xue, "Extended topological approach for the assessment of structural vulnerability in transmission networks," *IET Gener., Transmiss. Distrib.*, vol. 4, no. 6, pp. 716–724, Jun. 2010.

[17] E. Bompard, D. Wu, and F. Xue, "Structural vulnerability of power systems: A topological approach," *Electr. Power Syst. Res.*, vol. 81, no. 7, pp. 1334–1340, 2011.

[18] S. Poudel, Z. Ni, and W. Sun, "Electrical distance approach for searching vulnerable branches during contingencies," *IEEE Trans. Smart Grid*, vol. 9, no. 4, pp. 3373–3382, Jul. 2018.

[19] K. Wang, B. H. Zhang, Z. Zhang, X. G. Yin, and B. Wang, "An electrical betweenness approach for vulnerability assessment of power grids considering the capacity of generators and load," *Phys. A, Statist. Mech. Appl.*, vol. 390, nos. 23–24, pp. 4692–4701, 2011.

[20] L. Xu, X. Wang, and X. Wang, "Electric betweenness and its application in vulnerable line identification in power system," *Proc. CSEE*, vol. 30, no. 1, pp. 33–39, Jan. 2010.

[21] W. Liu, C. Liang, P. Xu, Y. Dan, J. Wang, and W. Wang, "Identification of critical line in power systems based on flow betweenness," *Proc. CSEE*, vol. 33, no. 31, pp. 90–98, Nov. 2013.

[22] A. Dwivedi and X. Yu, "A maximum-flow-based complex network approach for power system vulnerability analysis," *IEEE Trans. Ind. Informat.*, vol. 9, no. 1, pp. 81–88, Feb. 2013.

[23] J. Fang, C. Su, Z. Chen, H. Sun, and P. Lund, "Power system structural vulnerability assessment based on an improved maximum flow approach," *IEEE Trans. Smart Grid*, vol. 9, no. 2, pp. 777–785, Mar. 2018.

[24] H. George-Williams and E. Patelli, "Maintenance strategy optimization for complex power systems susceptible to maintenance delays and operational dynamics," *IEEE Trans. Rel.*, vol. 66, no. 4, pp. 1309–1330, Dec. 2017.

[25] H. George-Williams and E. Patelli, "Efficient availability assessment of reconfigurable multi-state systems with interdependencies," *Rel. Eng. Syst. Saf.*, vol. 165, pp. 431–444, Sep. 2017.

[26] T. Wang, X. Wei, T. Huang, J. Wang, H. Peng, M. J. Pérez-Jiménez, and L. Valencia-Cabrera, "Modeling fault propagation paths in power systems: A new framework based on event SNP systems with neurotransmitter concentration," *IEEE Access*, vol. 7, pp. 12798–12808, 2019.

[27] R. Rocchetta and E. Patelli, "Assessment of power grid vulnerabilities accounting for stochastic loads and model imprecision," *Int. J. Elect. Power Energy Syst.*, vol. 98, pp. 219–232, Jun. 2018.

[28] X. Zhang, L. Feng, Y. Rui, Z. Xuemin, M. Shengwei, Z. Zhen'an, and L. Xiaomeng, "Identification of key transmission lines in power grid using modified K-core decomposition," in *Proc. 3rd Int. Conf. Electr. Power Energy Convers. Syst.*, Istanbul, Turkey, Oct. 2013, pp. 1–6.

[29] P. D. H. Hines, I. Dobson, E. Cotilla-Sanchez, and M. Eppstein, "'Dual graph' and 'random chemistry' methods for cascading failure," in *Proc. 46th Hawaii Int. Conf. Syst. Sci.*, Wailea, Maui, HI, USA, Jan. 2013, pp. 2141–2150.

[30] X. Wei, S. Gao, T. Huang, E. Bompard, R. Pi, and T. Wang, "Complex network-based cascading faults graph for the analysis of transmission network vulnerability," *IEEE Trans. Ind. Informat.*, vol. 15, no. 3, pp. 1265–1276, Mar. 2019.

[31] X. Wei, J. Zhao, T. Huang, and E. Bompard, "A novel cascading faults graph based transmission network vulnerability assessment method," *IEEE Trans. Power Syst.*, vol. 33, no. 3, pp. 2995–3000, May 2018.

[32] X. Wei, S. Gao, T. Huang, T. Wang, and W. Fan, "Identification of two vulnerability features: A new framework for electrical networks based on the load redistribution mechanism of complex networks," *Complexity*, vol. 2019, Jan. 2019, Art. no. 3531209.

[33] Z. Ma, C. Shen, F. Liu, and S. Mei, "Fast screening of vulnerable transmission lines in power grids: A pagerank-based approach," *IEEE Trans. Smart Grid*, vol. 10, no. 2, pp. 1982–1991, Mar. 2019.

[34] F. Wenli, Z. Xuemin, M. Shengwei, H. Shaowei, W. Wei, and D. Lijie, "Vulnerable transmission line identification using ISH theory in power grids," *IET Gener., Transmiss. Distrib.*, vol. 12, no. 4, pp. 1014–1020, Feb. 2018.
[35] W.-L. Fan, X.-M. Zhang, S.-W. Mei, and S.-W. Huang, "Vulnerable transmission line identification considering depth of K-shell decomposition in complex grids," *IET Gener., Transmiss. Distrib.*, vol. 12, no. 5, pp. 1137–1144, Mar. 2018.
[36] R. Pi, Y. Cai, Y. Cao, and Y. Li, "Machine learning based on Bayes networks to predict the cascading failure propagation," *IEEE Access*, vol. 6, pp. 44815–44823, 2018.
[37] J. E. Hirsch, "An index to quantify an individual's scientific research output," *Proc. Nat. Acad. Sci. USA*, vol. 102, no. 46, pp. 16569–16572, 2005.
[38] L. Lü, T. Zhou, Q.-M. Zhang, and H. E. Stanley, "The H-index of a network node and its relation to degree and coreness," *Nature Commun.*, vol. 7, Jan. 2016, Art. no. 010168.
[39] B. A. Carreras, D. E. Newman, I. Dobson, and N. S. Degala, "Validating OPA with WECC data," in *Proc. 46th Hawaii Int. Conf. Syst. Sci.*, Wailea, Maui, HI, USA, Jan. 2013, pp. 2197–2205.
[40] Z. Ma, F. Liu, C. Shen, J. Zhang, and F. Gao, "Rapid identification of vulnerable lines in power grid using modified pagerank algorithm-Part I: Part II: Factors affecting identification results," *Proc. CSEE*, vol. 37, no. 1, pp. 36–44, 2017.
[41] F. Xiao and J. D. McCalley, "Power system risk assessment and control in a multiobjective framework," *IEEE Trans. Power Syst.*, vol. 24, no. 1, pp. 78–85, Feb. 2009.

QIAO ZHANG received the bachelor's degree in electrical engineering and its automation from Chongqing Jiaotong University, Chongqing, China. He is currently pursuing the master's degree with Southwest Jiaotong University, Chengdu, China. His research interest includes the vulnerability assessment of power systems.

WENLI FAN received the Ph.D. degree in power system and its automation from Southwest Jiaotong University, China, in 2014, where he is currently a Lecturer with the School of Electrical Engineering. His current research interests include power system analysis and control, especially power system complexity and security.

ZIYANG QIU received the bachelor's degree in electrical engineering from the Chongqing University of Posts and Telecommunications, Chongqing, China. He is currently pursuing the master's degree in electrical engineering with Southwest Jiaotong University, Chengdu, China. His research interests include the power system cascading failure modeling and blackout risk assessment.

ZHIGANG LIU (M'06–SM'16) received the Ph.D. degree in power system and automation from Southwest Jiaotong University, Chengdu, China, in 2003, where he is currently a Full Professor with the School of Electrical Engineering. His current research interests include electrical relationship of vehicle-grid in high-speed railways, power quality considering grid-connect of new energies, pantograph-catenary dynamics, fault detection, status assessment, and active control. He was elected as a fellow of the Institution of Engineering and Technology (IET) in 2017. He is an Associate Editor of the IEEE TRANSACTIONS ON INSTRUMENTATION AND MEASUREMENT, the IEEE TRANSACTIONS ON VEHICULAR TECHNOLOGY, and IEEE ACCESS.

JING ZHANG received the Ph.D. degree in mechanical manufacturing engineering and automation from Southwest Jiaotong University, Sichuan, China, in 2008, where she is currently an Associate Professor with the School of Electrical Engineering. Her current research interests include optimization design of pantograph- catenary parameters, aerodynamics of pantograph-catenary systems, and the control technology of high-speed pantograph.